Supplementary Information

Different Shapes Based on Ionic Liquid Leading to a Two-Stage Discharge Process

Kun Zhang[1,2], Guohui Zhou[1*], Timing Fang[1], Xiao Tang[1], Xiaomin Liu[1*]

1 School of Chemistry and Chemical Engineering, Qingdao University, Qingdao 266071, Shandong, China.

2 College of Materials Science and Engineering, Qingdao University, Qingdao 266071, Shandong, China.

* Corresponding author. E-mail: liuxiaomin@qdu.edu.cn, zhouguohui@126.com

1. Charge and Discharge

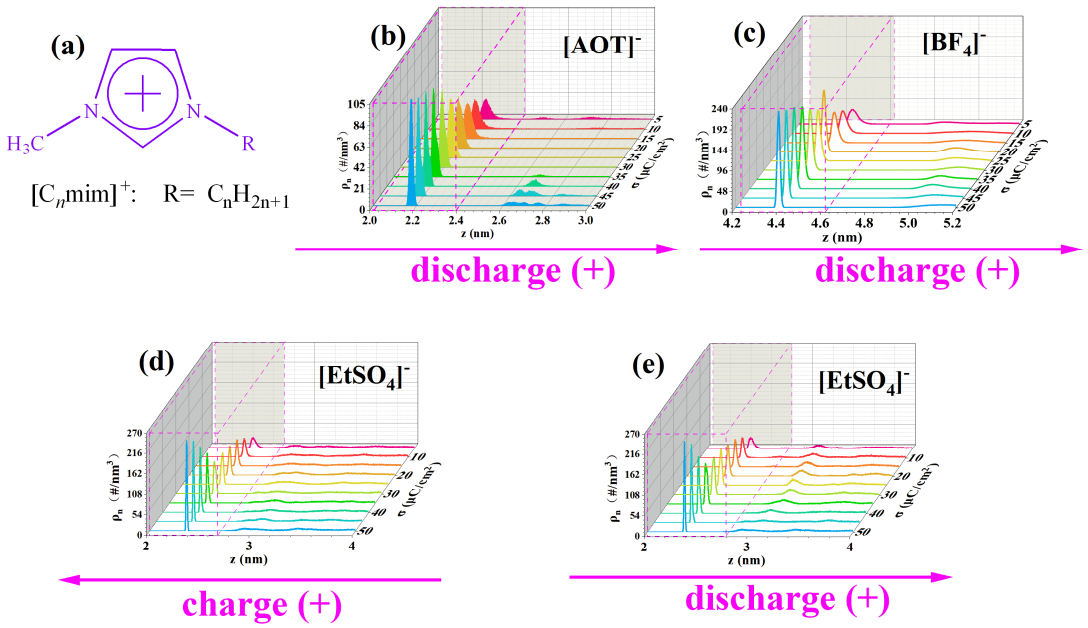

Fig S1. The charging and discharging process near positive electrode for different systems. (a) The $[C_n mim]^+$ structure, (b) ρ_n of sulfur atoms in $[C_6mim][AOT]$ during discharging process, (c) ρ_n of boron atoms in $[C_6mim][BF_4]^-$ during discharging process, (d) and (e) are ρ_n of sulfur atoms in $[C_2mim][EtSO_4]$ during the charging and discharging process, respectively.

The difference between charging and discharging near negative electrode are shown in Fig. 3a~d. For the $[C_n mim][AOT]$ system (n=4, 6 and 8), the number and proportion of i and j shapes grow faster and more orderly when σ= - 20~ - 35 μC/cm^2, which is order transition zone for the i and j-type cations, and the V-type anions (*J. Phys. Chem. Lett.* **2021**, *12*, 2273-2278). This is different from the two-stage discharging process. However, $[C_2mim][AOT]$ system do not have clear trend during the whole charging process, and its discharging process is an obviously two-stage discharging process.

We also investigated number density ρ_n of sulfur atoms in $[AOT]^-$, and the discharging process near positive electrode was also used as comparative studies near negative process. It can be seen that the process of discharge is similar to the reverse charging process near positive electrode for $[AOT]^-$ from the number density ρ_n between discharge (Fig. S1b) and charge (Fig. S2a).

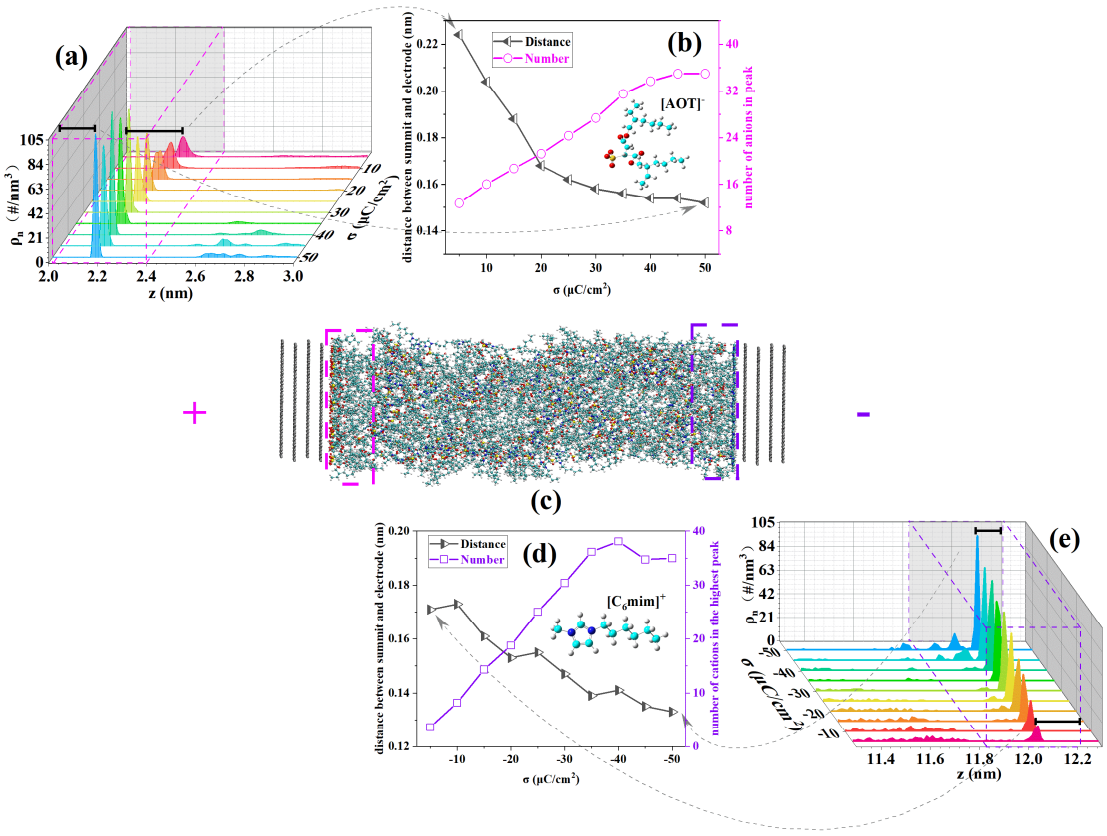

Fig S2. Boundary layer near positive and negative electrodes. Corresponding to $|\sigma|$= 5, 10, 15, 20, 25, 30, 35, 40, 45, 50μC/cm^2, (a) and (e) represent the number density ρ_n of sulfur atoms in $[AOT]^-$ and ρ_n of COM in imidazolium rings from $[C_6mim]^+$, respectively. In (b), the hollow magenta circle represents the number of anions in boundary layer which is drown in a magenta dash lines box in (a), and hollow bottom black triangle corresponds to the distance between the peak of ρ_n curve and electrode surface. In (e), hollow violet square represents the number of cations in highest peaks of boundary layer which is drown in a violet dash lines box (near 11.83 nm) in (d), and hollow top black triangle corresponds to the distance between the highest peak of ρ_n curve and electrode surface. (c) is the atomic structure of ILs-graphite interfaces (H, white; C, cyan; N, blue; S, yellow; O, red; the gray net layers represent an ideal graphite electrode).

2. Interaction Energy

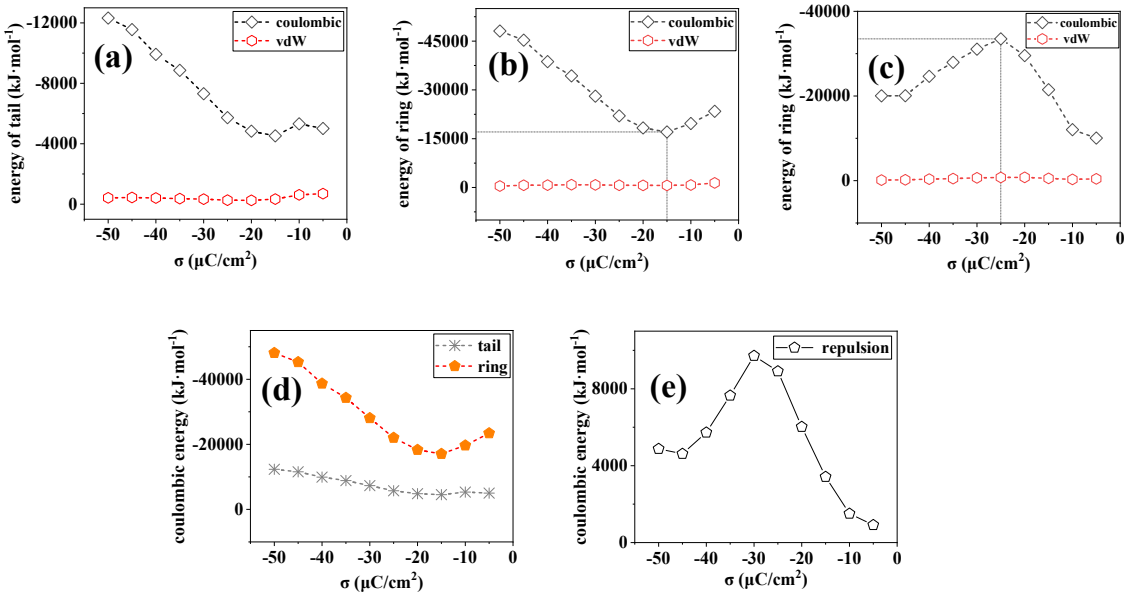

Fig S3. Interaction energy of rings and tails for $[C_6mim]^+$ during discharging. (a) Energy of tails in compact layer is from the negative electrode. (b) Energy of rings in compact layer is from the negative electrode. (c) Energy of rings in crowding layer is from the negative electrode. (d) Comparison of coulombic energy from the negative electrode to ring and tail in compact layer. (e) The repulsion is coulombic energy between crowding layer and compact layer.

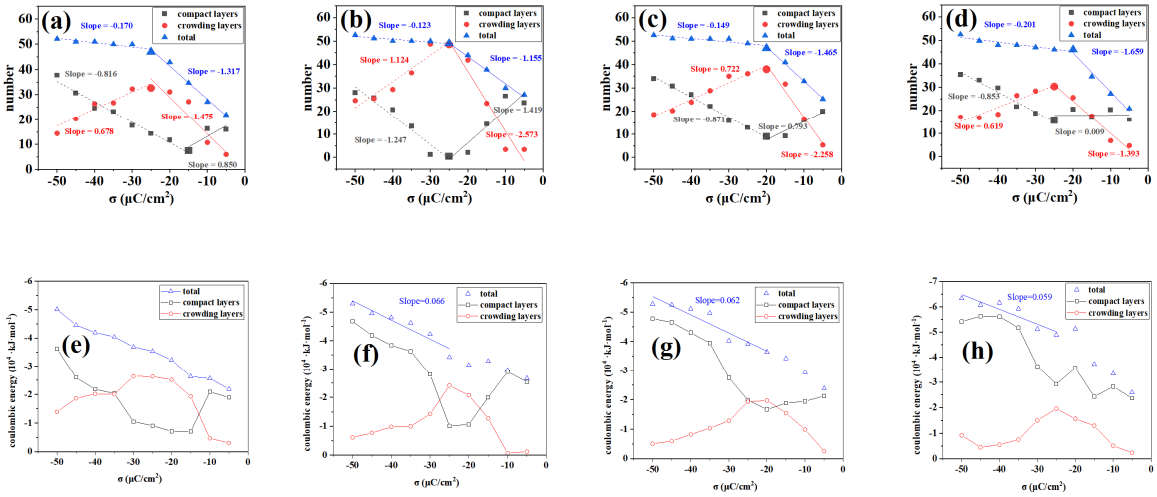

Fig S4. Contrast of increasing and decreasing rates from the slopes values. (a) is $[C_4mim]^+$ in system of $[C_4mim]$ [AOT]. (b), (c) and (d) are $[C_nmim]^+$ (n=2, 4 and 6, respectively) in system of $[C_nmim]$ $[BF_4]$. The blue symbols are total number in boundary layer near negative electrode. The red and black symbols are the cations number of crowding layers and compact layer. The coulombic energy in (e), (f), (g) and (h) are accumulative total of attraction and repulsion for imidazolium rings in (b), (c) and (d), respectively.

The number of cations moves from the compact layer into the crowding layer can be calculated by the reduction of cations in compact layer, its slope=$\triangle y/\triangle x$, where $\triangle y$ represents the number of cations move from compact layer into crowding layer, $\triangle x$ represents the surface charge density of electrode σ. When $\triangle x$ is 25 μC/cm^2, the $\triangle y$ for the $[C_nmim]$ $[BF_4]$ (n=2, 4, and 6) are 31.18, 21.78, and 21.33, respectively (Fig. S4b~d), and the $\triangle y$ for the $[C_nmim]$ [AOT](n=2, 4, and 6) are 25.88, 20.40 and 19.68, respectively (Fig. 4d, Fig. S4a, and Fig. 3e). So it can be concluded that the number of cations move from the compact layer into the crowding layer follows the order of $[C_2mim]^+ > [C_4mim]^+ > [C_6mim]^+$.

3. NAILs and SAILs

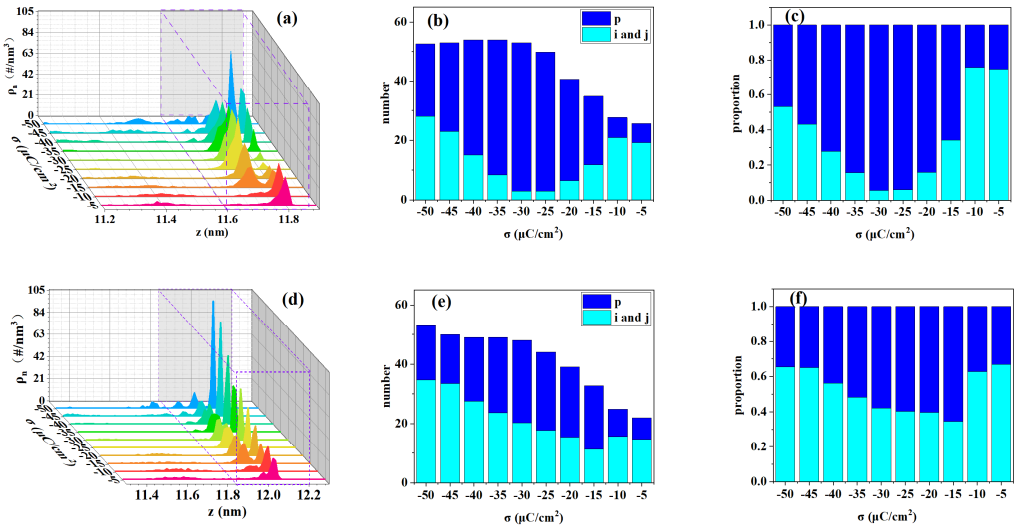

Fig S5. Discharging process for the [C$_n$mim][AOT] (n=2, 6) system in boundary layer with 100ns relaxation time for each |σ|. (a) and (d) is the number density ρ_n of $[C_2mim]^+$ and $[C_6mim]^+$ corresponding to COM of its imidazolium ring during discharging process, respectively. The (b) and (c) represent the $[C_2mim]^+$ cumulative number and proportion of p, i and j shape cations. The (e) and (f) represent the $[C_6mim]^+$ cumulative number and proportion of p, i and j shape cations. The (e) and (f) represent the $[C_6mim]^+$ cumulative number and proportion of p, i and j shape cations.

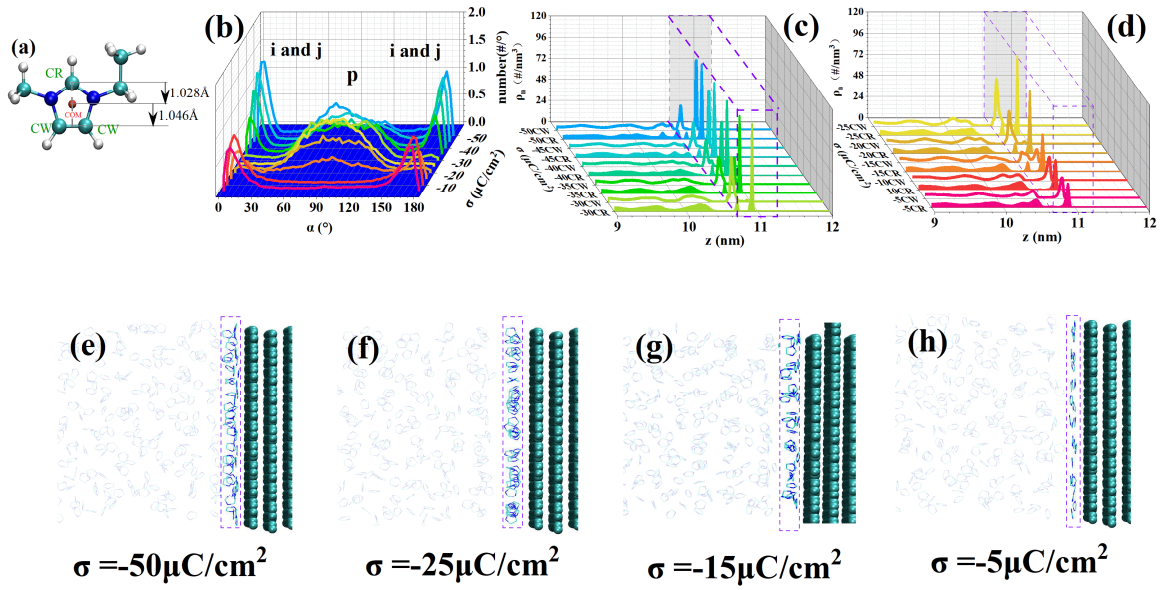

Fig S6. Standing and lying conformations of imidazolium rings of the $[C_2mim][BF_4]$ system during discharging. (a) is distance between CR atom and COM, and the distance between COM and bond of two CW atoms. (b) and (c) are the number density ρ_n of atom CR and one CW atom during discharging process. (d), (e) and (f) are the snapshots of discharging process for imidazolium rings in $|\sigma|$=-50, -25, -15 and -5μC/cm^2.

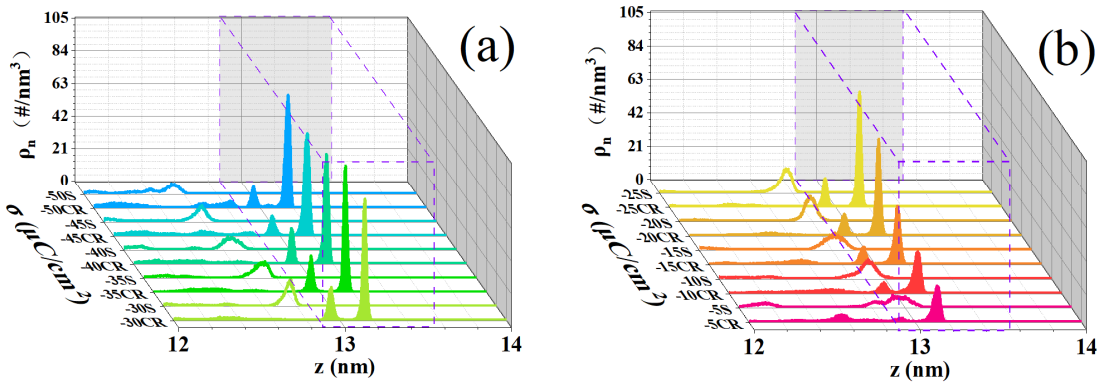

Fig S7. Discharging process for the [C_2mim][AOT] system in the boundary layer. The (a) and (b) are both the number density ρ_n of $[C_2mim]^+$ (which is represented by lines of the "CW" in Fig S7a), and number density ρ_n of $[AOT]^-$ (which is represented by solid peak shapes of the S atom for "S") during discharging process in molecular dynamics.

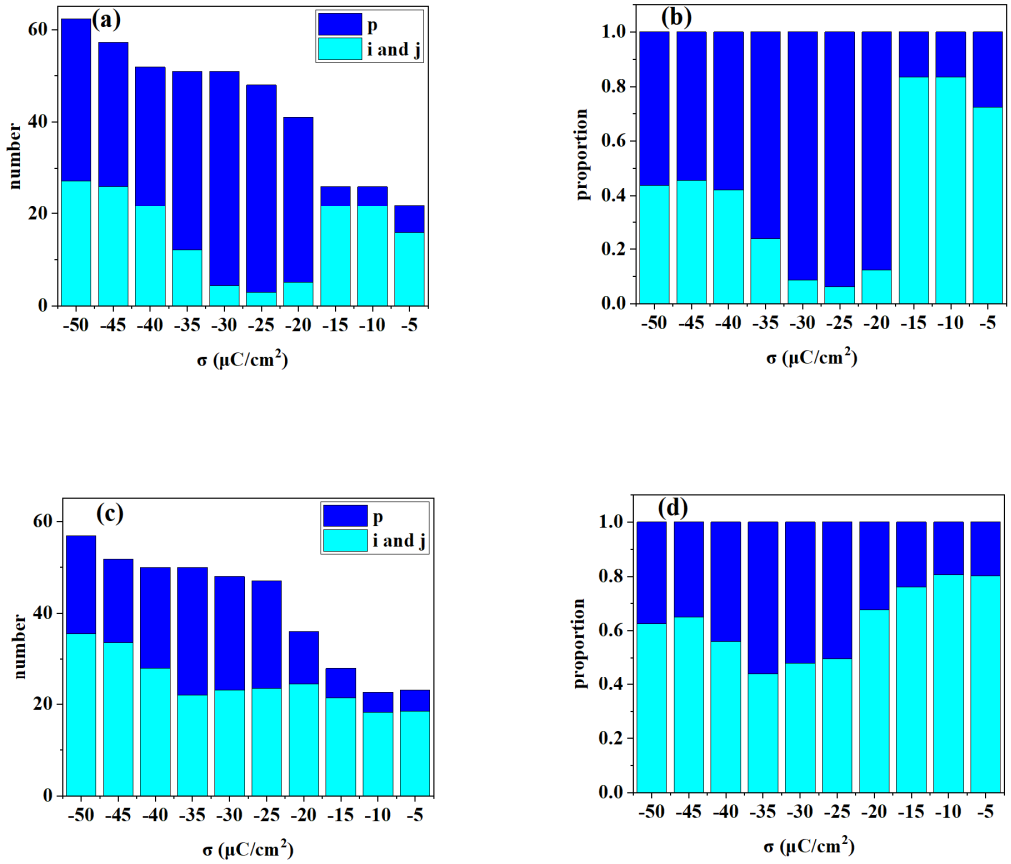

Fig S8. Discharging process for the [C$_n$mim][TFSI] (n=2, 6) system in the boundary layer. The (a) and (b) represent the [C$_2$mim]$^+$ cumulative number and proportion of p, i and j shape cations. The (c) and (d) represent the [C$_6$mim]$^+$ cumulative number and proportion of p, i and j shape cations.

The differences between [C$_2$mim][TFSI] system and [C$_2$mim][BF$_4$] system can be found by comparing Fig. 7a and Fig. S8a. The increasing trend for the number of [C$_2$mim]$^+$ is obviously different between these two systems during the second stage (σ= - 25~ - 5 μC/cm^2). [BF$_4$]$^-$ is smaller than [TFSI]$^-$, and the movement of the former is faster. [BF$_4$]$^-$ anions move into crowding layer earlier, which make some counterions standing (with p shape) in crowding layer for a longer time, and return (with i and j shapes) to the compact layer later. As a result, it can be seen in Fig. 7a ([C$_2$mim][BF$_4$] system), the number of i and j change slower than that in Fig. S8a ([C$_2$mim][TFSI] system) at the beginning of the second stage (σ= - 25~ - 15 μC/cm^2). The above results suggest that the second stage is a complex process, which is affected by the movement of both coions and counterions.